

Probing pure spin-rotation quantum geometry in persistent spin textures via nonlinear transport

Neelanjana Chakraborti,^{1,*} Akash Dey,^{2,3,*} Snehasish Nandy,^{4,†} Sudeep Kumar Ghosh^{1,‡} and Kush Saha^{5,2,3,§}

¹Department of Physics, Indian Institute of Technology, Kanpur 208016, India

²Department of Physics, National Institute of Science Education and Research, Jatni, 752050, India

³Homi Bhabha National Institute, Training School Complex, Anushakti Nagar, Mumbai 400094, India

⁴Department of Physics, National Institute of Technology Silchar, Assam 788010, India

⁵Max-Planck Institute for the Physics of Complex Systems, Noethnitzer Str. 38, 01187, Dresden, Germany

Persistent spin textures (PST) are spin-orbit coupled states in which Bloch spinors become momentum independent due to an underlying symmetry constraint, leading to the complete suppression of conventional and Zeeman quantum geometric tensor quantities. This makes accessing their intrinsic geometric structure experimentally challenging. Here, we show that the spin-rotation quantum geometric tensor (SRQGT) provides the missing probe. Using a two-dimensional electron gas and a cubic spin-splitting system as representative PST platforms, we demonstrate that the SRQGT remains finite and momentum independent and generates a measurable nonlinear gyrotropic current. The smoking-gun signature of PST is a fully direction-independent nonlinear gyrotropic response: magnetic currents coincide in magnitude and display identical parametric variations. These results establish PST systems as minimal platforms for isolating pure spin-rotation quantum geometry.

Persistent spin textures (PST) constitute a distinct regime of spin-orbit coupled systems in which spin dynamics are governed by an exact conserved spin projection [1, 2]. Initially identified in two-dimensional electron gases with balanced Rashba and Dresselhaus interactions, this condition stabilizes a persistent spin helix and dramatically enhances spin lifetimes [3]. Beyond this fine-tuned setting, related texture-preserving mechanisms have been shown to arise intrinsically in systems with cubic spin splitting [4] and in other symmetry-constrained band structures across the Brillouin zone [5, 6]. While such symmetry protection yields exceptional spin coherence, it also imposes stringent constraints on the structure of the eigenstates, making the internal quantum character of PST difficult to probe directly.

Quantum geometry, encoded in the quantum geometric tensor (QGT), provides a systematic framework for characterizing Bloch states [7, 8]. Its imaginary part defines the Berry curvature and its real part defines the quantum metric, which underlie anomalous transport [9–12], nonlinear optical responses [13], nonlinear Hall effects [14–16] and superconductivity [17–22]. In its conventional form, however, the QGT captures only momentum-space variations of the wavefunctions. Recent extensions for spin-orbit coupled systems have introduced a generalized QGT that incorporates spin-space rotations, yielding two additional QGTs: spin-rotation QGT (SRQGT) and Zeeman QGT [23, 24]. While the spin-rotation QGT accounts only spin rotation, the Zeeman QGT captures both spin rotations and momentum translation together. Remarkably, in a PST, the emergent SU(2) symmetry renders Bloch spinors momentum independent, causing the conventional QGT and Zeeman QGT to vanish identically throughout the Brillouin zone. This complete suppression of conventional and Zeeman QGTs raises a central question: can SRQGT provide a direct experimental

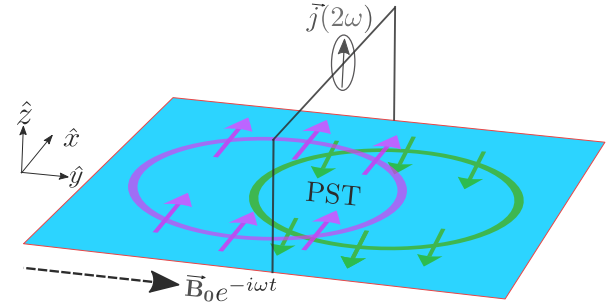


FIG. 1. Nonlinear Gyrotropic Magnetic Response in Persistent Spin Textures: Schematic of a persistent spin textures-hosting material subjected to a time-dependent magnetic field, where the leading response is a purely second-order gyrotropic magnetic current response arising entirely from the spin-rotation quantum geometry.

probe of PST?

In this paper, we show that PST systems provide minimal platforms to isolate spin-rotation quantum geometry via nonlinear transport, as schematically shown in Fig. 1. Examining a two-dimensional electron gas at the Rashba–Dresselhaus symmetry point and a purely cubic spin-splitting model as representative PST realizations, we find that conventional and Zeeman quantum geometric contributions vanish, whereas only the SRQGT remains finite and momentum independent. This residual geometry produces a nonlinear gyrotropic magnetic (NGM) current characterized by complete direction independence, with identical responses along all in-plane directions. A symmetry-preserving dispersion tilt further enables finite conduction NGM currents without disrupting the PST condition, establishing a clear transport signature of spin-rotation quantum geometry.

Nonlinear gyrotropic magnetic conductivity from spin-rotation quantum geometry: Quantum geometry conven-

tionally characterizes electronic wavefunctions through momentum-space variations. However, in spin-orbit coupled systems, a complete geometric description of Bloch states $|u_{m\mathbf{k}}^\zeta\rangle$ must also incorporate spin-space rotations [23], where ζ is the spin degrees of freedom. Assuming two-band model, a unified description of these generalized geometric quantities is obtained by defining the tensor $z_{mp}^{ab} = x_{mp}^a y_{pm}^b$, whose real and imaginary parts are $z_{mp}^{ab,R} = \frac{1}{2}(x_{mp}^a y_{pm}^b + x_{pm}^a y_{mp}^b)$ and $z_{mp}^{ab,I} = \frac{i}{2}(x_{mp}^a y_{pm}^b - x_{pm}^a y_{mp}^b)$, respectively; a and b refer to the spatial indices, and m, p denote band indices. By assigning the position (r) and Pauli spin (σ) operators to x and y , this unified formulation generates distinct geometric responses. Setting $x = y = r$ yields the conventional quantum metric \mathcal{G}_{mp}^{ab} and Berry curvature Ω_{mp}^{ab} [25–28], while the mixed choice $x = r, y = \sigma$ produces the Zeeman quantum metric \mathcal{Z}_{mp}^{ab} and corresponding Berry curvature \mathcal{F}_{mp}^{ab} [23, 29]. Crucially, choosing $x = y = \sigma$ defines the SRQGT, which decomposes into the spin-rotation quantum metric (SRQM) \mathcal{S}_{mp}^{ab} and spin-rotation Berry curvature (SRBC) Λ_{mp}^{ab} [30]. Under time-reversal (\mathcal{T}) and inversion (\mathcal{P}) symmetries, the SRQM remains even, whereas the SRBC is both \mathcal{T} -odd and \mathcal{P} -odd. This specific spin-rotation geometry directly governs the NGM current response to a time-varying magnetic field of frequency ω [31]. The total NGM conductivity separates into conduction (χ_{abc}^C) and displacement (χ_{abc}^D) contributions, driven respectively by the SRQM and SRBC:

$$\chi_{abc}^C = \left(\frac{g\mu_B}{2}\right)^2 \sum_{m \neq p} f_m \frac{\partial \epsilon_{mp}}{\partial k^a} \left(\frac{S_{mp}^{bc}}{\epsilon_{mp}^2}\right), \quad (1)$$

$$\chi_{abc}^D = \left(\frac{g\mu_B}{2}\right)^2 \sum_{m \neq p} f_m \frac{\partial \epsilon_{mp}}{\partial k^a} \left(\frac{\Lambda_{mp}^{bc}}{\hbar\omega\epsilon_{mp}}\right), \quad (2)$$

where f_m is the Fermi–Dirac distribution and $\epsilon_{mp} = \epsilon_m - \epsilon_p$ is the interband energy difference.

To demonstrate transport signatures of SRQGT for probing PST, we systematically calculate the generalized quantum geometry and the resulting nonlinear magnetic current responses for two distinct example systems:

i) *Two-dimensional electron gas (2DEG) where PST appears only at a symmetry-tuned point:* The Hamiltonian of a 2DEG in the presence of both Rashba (α) and Dresselhaus (β) type spin-orbit couplings is given by [32–35]

$$H = \frac{k^2}{2m} + \alpha(k_y\sigma_x - k_x\sigma_y) + \beta(k_x\sigma_x - k_y\sigma_y), \quad (3)$$

where the Pauli matrices σ operate on the spin space. This Hamiltonian preserves time-reversal (\mathcal{T}) symmetry but breaks inversion (\mathcal{P}) symmetry. For generic couplings ($\alpha \neq \beta$), the effective spin-orbit field $\mathcal{B}_{\text{eff}} = [\beta k_x + \alpha k_y, -(\alpha k_x + \beta k_y)]$ is momentum-dependent, producing anisotropic spin textures on the Fermi contours as depicted in Figs. 2(b) and (c). However, a fundamentally different regime emerges when $\alpha = \beta$. The effective field simplifies to $\mathcal{B}_{\text{eff}} = \alpha(k_x + k_y)(1, -1)$, rendering its

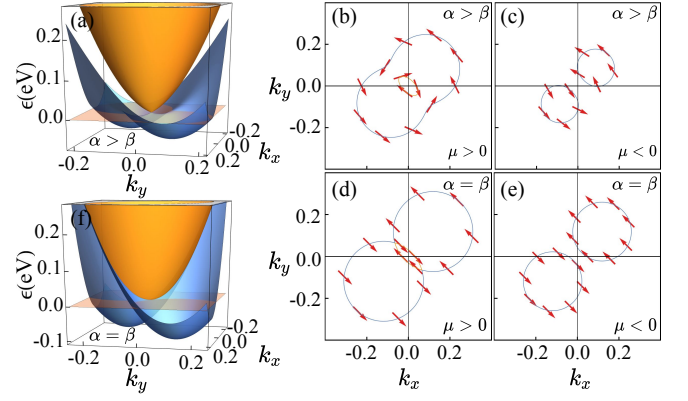


FIG. 2. **Spin Textures on Fermi Contours of a Rashba–Dresselhaus Two-Dimensional Electron Gas:** (a,f) Energy dispersions for $\alpha > \beta$ and $\alpha = \beta$. For $\alpha = 0.6$ eV.Å and $\beta = 0.2$ eV.Å, an isolated band-touching point lies on the zero-energy plane (orange). At $\alpha = \beta = 0.6$ eV.Å, a nodal line forms with its minimum touching the zero-energy plane. (b,d) Spin textures at fixed energy $\mu = 0.03$ eV for $\alpha > \beta$ and $\alpha = \beta$. (c,e) Corresponding spin textures at $\mu = -0.03$ eV.

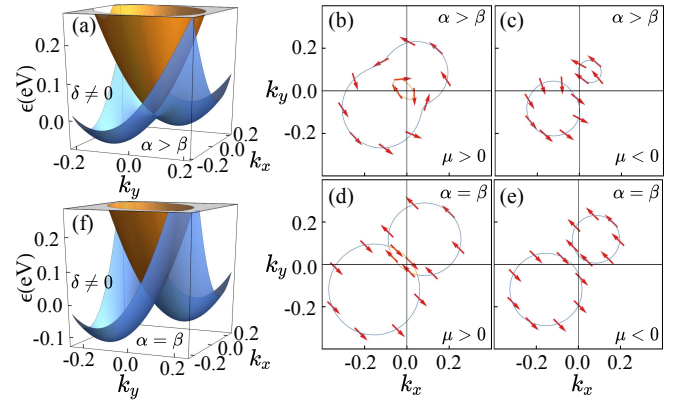


FIG. 3. **Spin Textures on Fermi Contours of a Rashba–Dresselhaus Two-Dimensional Electron Gas with Finite Tilt:** (a,f) Energy dispersions and spin textures in the presence of a tilt $\delta = 0.25$ eV.Å applied along k_x . (b,d) Spin textures at $\mu = 0.03$ eV for $\alpha > \beta$ and $\alpha = \beta$; (c,e) corresponding spin textures at $\mu = -0.03$ eV, showing that the tilt does not destroy the persistent spin textures.

direction momentum-independent and producing a unidirectional PST, as illustrated in Figs. 2(d) and (e) [5, 36].

We evaluate all components of the generalized geometric tensors associated with this system, the explicit expressions of which are provided in Table I. For $\alpha \neq \beta$, the strictly in-plane nature of the SOC field \mathcal{B}_{eff} precludes the emergence of $\Omega_{\pm\mp}^{ab}$, $\mathcal{Z}_{\pm\mp}^{ab}$, as well as the in-plane $\Lambda_{\pm\mp}^{xy}$ and the diagonal out-of-plane component $\Lambda_{\pm\mp}^{zz}$. Conversely, $\mathcal{G}_{\pm\mp}^{ab}$, $\mathcal{F}_{\pm\mp}^{ab}$, $\mathcal{S}_{\pm\mp}^{ab}$, and out-of-plane SRBC components, $\Lambda_{\pm\mp}^{xz}$, $\Lambda_{\pm\mp}^{yz}$, remain finite due to the anisotropic deformation of the Bloch states. Crucially, at the PST

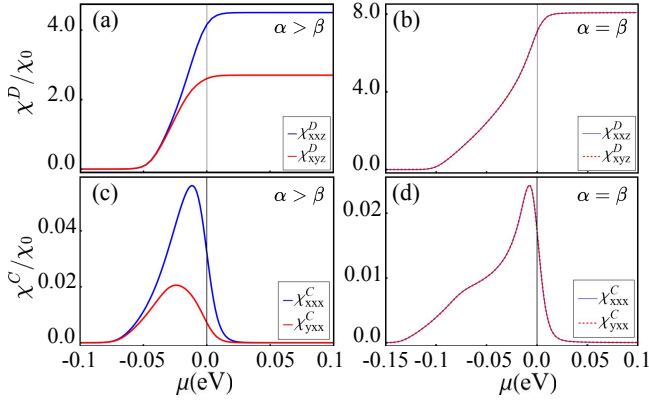


FIG. 4. **Displacement and Conduction Nonlinear Gyrotropic Magnetic Conductivity of Two-Dimensional Electron Gas:** (a, b) Only two of the non-vanishing displacement nonlinear gyrotropic magnetic conductivity components χ^D_{xxz} and χ^D_{yyz} are shown for $\alpha > \beta$ and $\alpha = \beta$, respectively. (c, d) The conduction nonlinear gyrotropic magnetic conductivity components χ^C_{xxx} and χ^C_{yxx} for $\alpha > \beta$ and $\alpha = \beta$, respectively in presence of tilt. We consider $T = 50$ K, $\omega = 10^{13}$ Hz and $\chi_0 = (\frac{g\mu_B}{2})^2 \text{ A}^{-1} \text{ m T}^2$.

point ($\alpha = \beta$), an exact emergent SU(2) symmetry arises [3, 37], simplifying the spin-orbit coupling to

$$H_{\text{SOC}}(\mathbf{k}) = \sqrt{2}\lambda(k_x + k_y)\Sigma, \quad (4)$$

where $\Sigma = (\sigma_x - \sigma_y)/\sqrt{2}$. Since Σ commutes with the Hamiltonian, the eigenstates are diagonal in the Σ basis, yielding the eigenvalues with $\zeta = \pm 1$:

$$E_{\zeta}(\mathbf{k}) = \frac{k^2}{2m} + \sqrt{2}\lambda\zeta|k_x + k_y|. \quad (5)$$

As a direct consequence, the spinor part of the Bloch eigenstates becomes entirely independent of the crystal momentum \mathbf{k} . The Berry connection thus vanishes identically, enforcing the strict suppression of all conventional and Zeeman geometric quantities. In striking contrast, the spin-rotation quantum metric $\mathcal{S}_{\pm\mp}^{ab}$ remain finite with a constant value of 1/2, while the out-of-plane SRBC becomes momentum-independent in magnitude:

$$\Lambda_{\pm\mp}^{yz} = \mp \frac{\sqrt{2}(k_x + k_y)}{|k_x + k_y|}. \quad (6)$$

Other components can be obtained from the Table I. This establishes the robust SRQGT as the sole surviving quantum geometric structure at the PST point.

Because the SRQGT dictates nonlinear transport, we analyze the displacement (χ^D) and conduction (χ^C) conductivities. For the time-reversal symmetric Hamiltonian in Eq. (3), the conduction current vanishes identically. This occurs because the momentum derivatives of the

interband energy,

$$\frac{\partial \epsilon_{+-}}{\partial k_x} = \frac{2k_x(\alpha^2 + \beta^2) + 4k_y\alpha\beta}{\sqrt{(\alpha k_x + \beta k_y)^2 + (\alpha k_y + \beta k_x)^2}}, \quad (7)$$

$$\frac{\partial \epsilon_{+-}}{\partial k_y} = \frac{2k_y(\alpha^2 + \beta^2) + 4k_x\alpha\beta}{\sqrt{(\alpha k_x + \beta k_y)^2 + (\alpha k_y + \beta k_x)^2}}, \quad (8)$$

is odd in \mathbf{k} , making the χ^C integrand odd over the Brillouin zone. The contributions from both bands vanish individually, since the Fermi function is an even function of k . In contrast, the integrand of χ^D is an even function of k and hence yields a finite contribution under integration over the entire Brillouin zone. This conclusion also holds for $\alpha = \beta$, i.e., at the PST point. Note that in Fig. 4(b), for PST ($\alpha = \beta$), both the displacement conductivity components become identical in contrast to non-PST ($\alpha \neq \beta$) (see Fig. 4(a)) because all the SRBC components have a similar functional form as Eq. (6).

For both PST and non-PST cases, the χ^D yields a finite response when $\mu < 0$, arising solely from a single band, as shown in Fig. 2(a) and (f). However, once μ crosses zero, both bands start contributing with opposite signs. These contributions cancel each other, resulting in an overall constant response. To activate a finite conduction response governed by the SRQM without destroying the underlying PST, we introduce a controlled dispersion tilt δk_x , breaking particle-hole and time-reversal symmetries while preserving the spin structure:

$$H_{\text{eff}} = \frac{k^2}{2m} + \alpha(k_y\sigma_x - k_x\sigma_y) + \beta(k_x\sigma_x - k_y\sigma_y) + \delta k_x, \quad (9)$$

yielding the asymmetric dispersion

$$\epsilon_{\pm} = \frac{k^2}{2m} + \delta k_x \pm \sqrt{(\alpha k_x + \beta k_y)^2 + (\alpha k_y + \beta k_x)^2}. \quad (10)$$

As shown in Fig. 3, this tilt produces asymmetric Fermi contours, lifting the perfect cancellation between opposite momentum states.

For generic couplings ($\alpha \neq \beta$), the resulting conduction tensor components (e.g., χ^C_{xxx} and χ^C_{yxx}) are distinct due to the anisotropic SRQM components (Fig. 4(c)). However, the smoking-gun signature of the PST emerges exactly at $\alpha = \beta$: because the SRQM is a nonzero constant, the NGM conductivities become completely direction-independent, forcing all non-vanishing magnetic current response components to become perfectly identical (Fig. 4(d)).

The finite behavior of χ^C in the presence of tilt can further be understood from the dispersion shown in the subfigure (a) and (f) of Fig. 3. For $\epsilon_{\min} \leq \mu \leq \epsilon_{\text{BTP}}$, the lowest band exhibits two Fermi contours with opposite spin orientations at a fixed energy, and hence solely contributes to χ . For $\delta = 0$, these Fermi contours are

symmetric (see Fig. 2(c) and (e)), leading to vanishing net response. In contrast, for $\delta \neq 0$, the Fermi contours become asymmetric (see Fig. 3(c) and (e)), resulting in a finite χ .

For $\mu > \epsilon_{\text{BTP}}$, both the bands contribute to χ^C . For a fixed energy, the spin orientations in these two bands are opposite to each other, as evident from Fig. 2(b) and (d). However, when $\delta = 0$, the symmetry of the Fermi contours ensures that the contributions from the two bands cancel, yielding zero net response. For finite δ , the asymmetry of the Fermi contours again produces a finite χ , similar to the case $\mu < \epsilon_{\text{BTP}}$ (see Fig. 3(b) and (d)). However, as μ becomes sufficiently large, the contributions from the two contours tend to become equal in magnitude but opposite in sign, leading to an overall cancellation and hence a vanishing response at higher μ . These behaviors hold for both $\alpha = \beta$ and $\alpha \neq \beta$ cases. Such transport signatures can be probed in non-centrosymmetric semiconductor quantum wells, such as GaAs/AlGaAs or InAs-based heterostructures [33–35].

ii) *System with purely cubic spin splittings where the PST is robust throughout the Brillouin zone:* We further corroborate this unique geometric isolation by examining a system exhibiting purely cubic spin splittings, which hosts an intrinsic, symmetry-protected PST [4]. The effective two-band Hamiltonian is

$$H(\mathbf{k}) = E_0 + \Delta(k_x^2 + k_y^2) + \left[\zeta k_x(k_x^2 - 3k_y^2) + \lambda k_y(3k_x^2 - k_y^2) \right] \sigma_z, \quad (11)$$

yielding the energy dispersion

$$E_{\pm}(\mathbf{k}) = E_0 + \Delta(k_x^2 + k_y^2) \pm \left| \zeta k_x(k_x^2 - 3k_y^2) + \lambda k_y(3k_x^2 - k_y^2) \right|. \quad (12)$$

Because the spin-dependent term is strictly proportional to σ_z , the spin orientation remains fixed out-of-plane throughout the Brillouin zone, realizing a PST entirely independent of the specific parameters ζ and λ (the inset of Fig. 5(b)). Just as in the 2DEG model at the PST point, the eigenstates here are inherently momentum-independent. Accordingly, the Berry connection therefore vanishes identically, resulting in the strict suppression of $\mathcal{G}_{\pm\mp}^{ab}$, $\Omega_{\pm\mp}^{ab}$, $\mathcal{Z}_{\pm\mp}^{ab}$, and $\mathcal{F}_{\pm\mp}^{ab}$. The SRQGT again emerges as the unique geometric probe. The SRBC ($\Lambda_{\pm\mp}^{ab}$) and the SRQM ($\mathcal{S}_{\pm\mp}^{ab}$) remain finite and momentum-independent:

$$\Lambda_{\pm\mp}^{xy} = -\Lambda_{\pm\mp}^{yx} = \pm 2, \quad \mathcal{S}_{\pm\mp}^{xx} = \mathcal{S}_{\pm\mp}^{yy} = 1.$$

Remarkably, at the PST point, the formally time-reversal-odd SRBC effectively behaves as a pseudo time-reversal-even quantity due to this momentum-independence.

Analyzing the transport responses, the interband en-

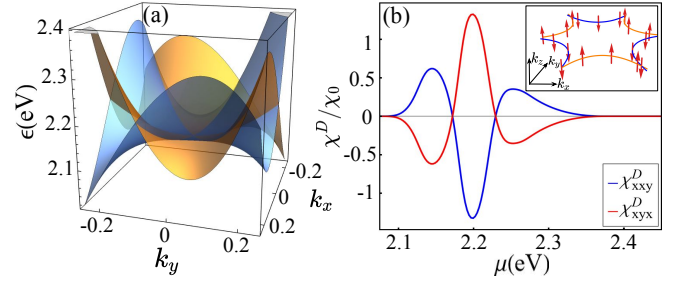


FIG. 5. **Spin Textures and Displacement Magnetic Current Response in a System with Purely Cubic Spin Splittings:** (a) Energy dispersion. (b) Two of the nonvanishing components of the displacement nonlinear gyrotropic magnetic conductivity, χ_{xxy}^D and χ_{xyx}^D ; inset: spin textures along the Fermi contours. Parameters: $E_0 = 2.13$ eV, $\Delta = 1.27$ eV $\cdot\text{\AA}^2$, $\zeta = -5.24$ eV $\cdot\text{\AA}^3$, $\lambda = -3.43$ eV $\cdot\text{\AA}^3$, $T = 50$ K and $\omega = 10^{13}$ Hz.

ergy derivatives for this cubic system read

$$\frac{\partial \epsilon_{+-}}{\partial k_x} = 3\zeta(k_x^2 - k_y^2) + 6\lambda k_x k_y, \quad (13)$$

$$\frac{\partial \epsilon_{+-}}{\partial k_y} = -6\zeta k_x k_y + 3\lambda(k_x^2 - k_y^2). \quad (14)$$

Since $\epsilon_+(\mathbf{k}) = \epsilon_-(-\mathbf{k})$, the Fermi-function difference is an odd function of \mathbf{k} . Combined with the constant SRQM and even energy derivatives, the conduction integrand becomes odd and vanishes identically upon integration. However, time-reversal symmetry permits a finite displacement current driven entirely by the SRBC. The contributions from the two bands cancel each other exactly, in contrast to the 2DEG system, where the contribution from each band vanishes individually. The resulting displacement conductivities (e.g., χ_{xxy}^D and χ_{xyx}^D , shown in Fig. 5(b)) mirror the simplicity of the underlying geometry, experiencing strong enhancement as the chemical potential approaches the band-touching points near $\mu = 2.2$ eV can be seen from Fig. 5(a)). This purely cubic model, realizable in layered transition-metal dichalcogenides lacking inversion symmetry [4], confirms that the SRQGT provides the exclusive transport signature of persistent spin textures.

The central result of this work is that the PST regime realizes a quantum-geometric phase in which the SRQGT constitutes the only surviving quantum geometric sector. At the PST point, the \mathbf{k} -independence of the Bloch spinors forces the conventional and Zeeman quantum metrics and corresponding Berry curvatures to vanish. In contrast, SRQM and SRBC remain finite constants originating purely from spin-space structure. This separation is explicitly demonstrated in both the 2DEG at $\alpha = \beta$ and the purely cubic model. While time-reversal symmetry restricts the response to displacement currents, a controlled symmetry-preserving dispersion tilt activates finite conduction contributions. At PST, the nonlinear

transport tensor collapses to identical components, yielding a fully isotropic response governed solely by the underlying SRQGT.

This geometric regime is experimentally accessible across multiple platforms. In solid-state systems, the required dispersion tilt can be engineered using unidirectional strain, in-plane potential gradients, or structural asymmetry in quantum wells [38–42]. Cold-atom realizations with synthetic spin–orbit coupling offer an even more tunable setting, where both the PST condition and controlled tilts can be implemented via Raman coupling schemes [43–45]. Beyond transport, SRQM and SRBC can be directly extracted through spin-fidelity protocols, Ramsey interferometry, or short-time quench dynamics [46–55]. Because these geometric quantities are momentum independent in the PST regime, they remain robust against thermal averaging, providing an unusually clean experimental probe.

In summary, PST isolates spin-rotation quantum geometry by symmetry, removing all momentum-space geometric contributions while preserving finite SRQM and SRBC that directly control macroscopic response. This establishes the SRQGT as a measurable physical quantity rather than a formal construct and positions PST as a minimal platform for exploring generalized quantum geometry and its applications in spintronics and coherent transport.

Acknowledgments: KS thanks J Mitcherling for useful discussions. N. C. and AD acknowledge the Council of Scientific and Industrial Research (CSIR), Government of India, for providing the SRF fellowship. S. K. G. and S. N. acknowledge financial support from Anusandhan National Research Foundation (ANRF) erstwhile Science and Engineering Research Board (SERB), Government of India respectively via the Startup Research Grant: SRG/2023/000934 and the Prime Minister’s Early Career Research Grant: ANRF/ECRG/2024/005947/PMS. KS acknowledge financial support from the Department of Atomic Energy (DAE), Govt. of India, through the project Basic Research in Physical and Multidisciplinary Sciences via RIN4001.

Quantum geometric quantities for the Rashba-Dresselhaus system

The analytical expressions for the different QGT components of the 2DEG system, in which PST emerges only at a symmetry-tuned point, are given in Table I.

QGT	Expression
$\mathcal{G}_{\pm\mp}^{xx}$	$\pm \frac{k_y^2 (\alpha^2 - \beta^2)^2}{[4k_x k_y \alpha \beta + k_x^2 (\alpha^2 + \beta^2) + k_y^2 (\alpha^2 + \beta^2)]^2}$
$\mathcal{G}_{\pm\mp}^{yy}$	$\mp \frac{k_x^2 (\alpha^2 - \beta^2)^2}{[4k_x k_y \alpha \beta + k_x^2 (\alpha^2 + \beta^2) + k_y^2 (\alpha^2 + \beta^2)]^2}$
$\mathcal{G}_{\pm\mp}^{xy} = \mathcal{G}_{\mp\pm}^{yx}$	$\pm \frac{k_x k_y (\alpha^2 - \beta^2)^2}{[4k_x k_y \alpha \beta + k_x^2 (\alpha^2 + \beta^2) + k_y^2 (\alpha^2 + \beta^2)]^2}$
$\Omega_{\pm\mp}^{ab}$	0
$\mathcal{Z}_{\pm\mp}^{ab}$	0
$\mathcal{F}_{\pm\mp}^{xy}$	$\pm \frac{k_y (\alpha^2 - \beta^2) (\alpha k_x + \beta k_y)}{[4k_x k_y \alpha \beta + k_x^2 (\alpha^2 + \beta^2) + k_y^2 (\alpha^2 + \beta^2)]^{3/2}}$
$\mathcal{F}_{\pm\mp}^{yx}$	$\mp \frac{k_x (\alpha^2 - \beta^2) (\alpha k_x + \beta k_y)}{[4k_x k_y \alpha \beta + k_x^2 (\alpha^2 + \beta^2) + k_y^2 (\alpha^2 + \beta^2)]^{3/2}}$
$\mathcal{F}_{\pm\mp}^{xx}$	$\pm \frac{k_y (\alpha^2 - \beta^2) (\alpha k_x + \beta k_y)}{[4k_x k_y \alpha \beta + k_x^2 (\alpha^2 + \beta^2) + k_y^2 (\alpha^2 + \beta^2)]^{3/2}}$
$\mathcal{F}_{\pm\mp}^{yy}$	$\mp \frac{k_x (\alpha^2 - \beta^2) (\alpha k_x + \beta k_y)}{[4k_x k_y \alpha \beta + k_x^2 (\alpha^2 + \beta^2) + k_y^2 (\alpha^2 + \beta^2)]^{3/2}}$
$\mathcal{S}_{\pm\mp}^{xx}$	$\frac{(k_x \alpha + k_y \beta)^2}{4k_x k_y \alpha \beta + k_x^2 (\alpha^2 + \beta^2) + k_y^2 (\alpha^2 + \beta^2)}$
$\mathcal{S}_{\pm\mp}^{yy}$	$\frac{(k_y \alpha + k_x \beta)^2}{4k_x k_y \alpha \beta + k_x^2 (\alpha^2 + \beta^2) + k_y^2 (\alpha^2 + \beta^2)}$
$\mathcal{S}_{\pm\mp}^{xy} = \mathcal{S}_{\mp\pm}^{yx}$	$\frac{(k_y \alpha + k_x \beta) (k_x \alpha + k_y \beta)}{4k_x k_y \alpha \beta + k_x^2 (\alpha^2 + \beta^2) + k_y^2 (\alpha^2 + \beta^2)}$
$\mathcal{S}_{\pm\mp}^{zz}$	1
$\Lambda_{\pm\mp}^{xy} = \Lambda_{\mp\pm}^{yx}$	0
$\Lambda_{\pm\mp}^{zz}$	0
$\Lambda_{\pm\mp}^{xz} = \Lambda_{\mp\pm}^{zx}$	$\mp \frac{2(k_x \alpha + k_y \beta)}{\sqrt{4k_x k_y \alpha \beta + k_x^2 (\alpha^2 + \beta^2) + k_y^2 (\alpha^2 + \beta^2)}}$
$\Lambda_{\pm\mp}^{yz} = \Lambda_{\mp\pm}^{zy}$	$\mp \frac{2(k_y \alpha + k_x \beta)}{\sqrt{4k_x k_y \alpha \beta + k_x^2 (\alpha^2 + \beta^2) + k_y^2 (\alpha^2 + \beta^2)}}$

TABLE I. Analytical expressions of different components of the QGTs for the Rashba–Dresselhaus 2DEG.

- [1] J. Schliemann, Colloquium: Persistent spin textures in semiconductor nanostructures, *Rev. Mod. Phys.* **89**, 011001 (2017).
- [2] J. Schliemann and D. Loss, Anisotropic transport in a two-dimensional electron gas in the presence of spin-orbit coupling, *Phys. Rev. B* **68**, 165311 (2003).
- [3] B. A. Bernevig, J. Orenstein, and S.-C. Zhang, Exact su(2) symmetry and persistent spin helix in a spin-orbit coupled system, *Phys. Rev. Lett.* **97**, 236601 (2006).
- [4] H. J. Zhao, H. Nakamura, R. Arras, C. Paillard, P. Chen, J. Gosteau, X. Li, Y. Yang, and L. Bellaiche, Purely cubic spin splittings with persistent spin textures, *Phys. Rev. Lett.* **125**, 216405 (2020).
- [5] L. L. Tao and E. Y. Tsymlal, Persistent spin texture enforced by symmetry, *Nature Communications* **9**, 2763

* These authors contributed equally

† snehasish@phy.nits.ac.in

‡ skghosh@iitk.ac.in

§ kush.saha@niser.ac.in

- (2018).
- [6] B. Kilic, S. Alvarruiz, E. Barts, B. van Dijk, P. Barone, and J. Sławińska, Universal symmetry-protected persistent spin textures in noncentrosymmetric crystals, *Nature Communications* **16**, 7999 (2025).
- [7] J. P. Provost and G. Vallee, Riemannian structure on manifolds of quantum states, *Communications in Mathematical Physics* **76**, 289 (1980).
- [8] M. V. Berry, Quantal phase factors accompanying adiabatic changes, *Proceedings of the Royal Society A* **392**, 45 (1984).
- [9] J. Mitscherling, Longitudinal and anomalous hall conductivity of a general two-band model, *Phys. Rev. B* **102**, 165151 (2020).
- [10] A. Avdoshkin, J. Mitscherling, and J. E. Moore, Multi-state geometry of shift current and polarization, *Phys. Rev. Lett.* **135**, 066901 (2025).
- [11] O. Antebi, J. Mitscherling, and T. Holder, Drude weight of an interacting flat-band metal, *Phys. Rev. B* **110**, L241111 (2024).
- [12] J. Mitscherling and T. Holder, Bound on resistivity in flat-band materials due to the quantum metric, *Phys. Rev. B* **105**, 085154 (2022).
- [13] A. Postlewaite, A. Raj, S. Chaudhary, and G. A. Fiete, Quantum geometry and nonlinear optical responses in rhombohedral trilayer graphene, *Phys. Rev. B* **110**, 245122 (2024).
- [14] Y. Ulrich, J. Mitscherling, L. Classen, and A. P. Schnyder, Quantum geometric origin of the intrinsic nonlinear hall effect, *arXiv preprint arXiv:2506.17386* (2025).
- [15] A. Dey, Nonlinear hall responses in tunable nodal dirac semimetals (2025), *arXiv:2511.20214* [cond-mat.mes-hall].
- [16] S. Sarkar, S. Das, and A. Agarwal, Symmetry-driven intrinsic nonlinear pure spin hall effect (2025), *arXiv:2502.18226* [cond-mat.mes-hall].
- [17] S. Peotta and P. Törmä, Superfluidity in topologically nontrivial flat bands, *Nature Communications* **6**, 8944 (2015).
- [18] L. Liang, T. I. Vanhala, S. Peotta, T. Siro, A. Harju, and P. Törmä, Band geometry, berry curvature and superfluid weight, *Physical Review B* **95**, 024515 (2017).
- [19] L. Xiang, H. Jin, and J. Wang, Spin transport revealed by spin quantum geometry, *Phys. Rev. Lett.* **135**, 146303 (2025).
- [20] L. Xiang, J. Jia, F. Xu, and J. Wang, Classification of electromagnetic responses by quantum geometry (2025), *arXiv:2510.02661* [cond-mat.mes-hall].
- [21] J. Iguchi, H. Watanabe, Y. Murakami, T. Nomoto, and R. Arita, Bulk photovoltaic effect in antiferromagnet: Role of collective spin dynamics, *Phys. Rev. B* **109**, 064407 (2024).
- [22] K. Hattori, H. Watanabe, and R. Arita, Nonlinear hall effect driven by spin-charge-coupled motive force, *Phys. Rev. B* **111**, 174416 (2025).
- [23] L. Xiang, J. Jia, F. Xu, Z. Qiao, and J. Wang, Intrinsic gyrotropic magnetic current from zeeman quantum geometry, *Phys. Rev. Lett.* **134**, 116301 (2025).
- [24] N. Chakraborti, S. K. Ghosh, and S. Nandy, Zeeman quantum geometry as a probe of unconventional magnetism (2025), *arXiv:2508.14745* [cond-mat.mes-hall].
- [25] D. Xiao, M.-C. Chang, and Q. Niu, Berry phase effects on electronic properties, *Rev. Mod. Phys.* **82**, 1959 (2010).
- [26] Y. Jiang, T. Holder, and B. Yan, Revealing quantum geometry in nonlinear quantum materials, *Reports on Progress in Physics* **88**, 076502 (2025).
- [27] Y. Gao, S. A. Yang, and Q. Niu, Field induced positional shift of bloch electrons and its dynamical implications, *Phys. Rev. Lett.* **112**, 166601 (2014).
- [28] Z. Z. Du, H.-Z. Lu, and X. C. Xie, Nonlinear hall effects, *Nature Reviews Physics* **3**, 744 (2021).
- [29] N. Chakraborti, S. Nandy, and S. K. Ghosh, Gyrotropic fingerprints of magnetic topological insulator-unconventional magnet interfaces (2025), *arXiv:2512.18621* [cond-mat.mes-hall].
- [30] J. Jia, L. Xiang, Z. Qiao, and J. Wang, Nonlinear magnetoelectric edelstein effect (2025), *arXiv:2507.23415* [cond-mat.mes-hall].
- [31] N. Chakraborti, S. Nandy, and S. K. Ghosh, Intrinsic nonlinear gyrotropic magnetic effect governed by spin-rotation quantum geometry (2026), *arXiv:2601.22019* [cond-mat.mes-hall].
- [32] X. Cartoixa, L.-W. Wang, D.-Y. Ting, and Y.-C. Chang, Higher-order contributions to rashba and dresselhaus effects, *Phys. Rev. B* **73**, 205341 (2006).
- [33] Y. A. Bychkov and E. I. Rashba, Oscillatory effects and the magnetic susceptibility of carriers in inversion layers, *J. Phys. C* **17**, 6039 (1984).
- [34] G. Dresselhaus, Spin-orbit coupling effects in zinc blende structures, *Phys. Rev.* **100**, 580 (1955).
- [35] R. Winkler, *Spin-Orbit Coupling Effects in Two-Dimensional Electron and Hole Systems* (Springer, 2003).
- [36] A. Dey, A. K. Nandy, and K. Saha, Current-induced spin polarisation in rashba-dresselhaus systems under different point groups, *New Journal of Physics* **27**, 013024 (2025).
- [37] J. Schliemann, J. C. Egues, and D. Loss, Nonballistic spin-field-effect transistor, *Physical Review Letters* **90**, 146801 (2003).
- [38] S. D. Ganichev, V. V. Bel'kov, P. Schneider, E. L. Ivchenko, S. A. Tarasenko, W. Wegscheider, D. Weiss, and W. Prettl, Spin-galvanic effect, *Physical Review Letters* **90**, 136801 (2003).
- [39] D. A. B. Miller, D. S. Chemla, T. C. Damen, A. C. Gosard, W. Wiegmann, T. H. Wood, and C. A. Burrus, Band-edge electroabsorption in quantum well structures: The quantum-confined stark effect, *Physical Review Letters* **53**, 2173 (1984).
- [40] H. Ye, C. Hu, G. Wang, H. Zhao, H. Tian, W. Wang, and B. Liu, Anisotropic in-plane spin splitting in an asymmetric (001) gaas/algaas quantum well, *Nanoscale Research Letters* **6**, 520 (2011).
- [41] R. R. Binder, B. B. Gu, and N. H. Kwong, Quantum-confined strain gradient effect in semiconductor nanomembranes, *Physical Review B* **90**, 195208 (2014).
- [42] P. S. Grigoryev, A. S. Kurdyubov, M. S. Kuznetsova, Y. P. Efimov, S. A. Eliseev, V. V. Petrov, V. A. Lovtcius, P. Y. Shapochkin, and I. V. Ignatiev, Excitons in asymmetric quantum wells, *arXiv:1602.03720* (2016), *arXiv preprint*, 1602.03720.
- [43] Y.-J. Lin, K. Jiménez-García, and I. B. Spielman, Spin-orbit-coupled bose-einstein condensates, *Nature* **471**, 83 (2011).
- [44] I. B. Spielman, Raman-induced spin-orbit coupling in ultracold fermi gases, *Physical Review A* **79**, 063613 (2009).

- [45] J. D. Koralek, C. P. Weber, J. Orenstein, B. A. Bernevig, S.-C. Zhang, S. Mack, and D. D. Awschalom, Emergence of the persistent spin helix in semiconductor quantum wells, *Nature* **458**, 610 (2009).
- [46] V. Gritsev and A. Polkovnikov, Nonequilibrium dynamics of quantum systems: Order parameter oscillations and quantum geometry, *PNAS* **109**, 6457 (2012).
- [47] M. Kolodrubetz, D. Sels, P. Mehta, and A. Polkovnikov, Geometry and non-adiabatic response in quantum and classical systems, *Physics Reports* **697**, 1 (2017).
- [48] P. Harvey-Collard, B. D'Anjou, M. Rudolph, N. T. Jacobson, J. Dominguez, G. A. Ten Eyck, J. R. Wendt, T. Pluym, M. P. Lilly, W. A. Coish, M. Pioro-Ladrière, and M. S. Carroll, High-fidelity single-shot readout for a spin qubit via an enhanced latching mechanism, *Phys. Rev. X* **8**, 021046 (2018).
- [49] H. Kiyama, D. van Hien, A. Ludwig, A. D. Wieck, and A. Oiwa, High-fidelity spin readout via the double latching mechanism, *npj Quantum Information* **10**, 95 (2024).
- [50] N. F. Ramsey, A molecular beam resonance method with separated oscillating fields, *Physical Review* **78**, 695 (1950).
- [51] M. Atala, M. Aidelsburger, J. T. Barreiro, D. Abanin, T. Kitagawa, E. Demler, and I. Bloch, Direct measurement of the zak phase in topological bloch bands, *Nature Physics* **9**, 795 (2013).
- [52] C. Godfrin, R. Ballou, E. Bonet, M. Ruben, S. Klyatskaya, W. Wernsdorfer, and F. Balestro, Generalized ramsey interferometry explored with a single nuclear spin qudit, *npj Quantum Information* **4**, 53 (2018).
- [53] D. Hu, L. Niu, S. Jin, X. Chen, G. Dong, J. Schmiedmayer, and X. Zhou, Ramsey interferometry with trapped motional quantum states, *Communications Physics* **1**, 29 (2018).
- [54] X. Tan, D.-W. Zhang, Z. Yang, J. Chu, Y.-Q. Zhu, D. Li, X. Yang, S. Song, Z. Han, Z. Li, Y. Dong, H.-F. Yu, H. Yan, S.-L. Zhu, and Y. Yu, Experimental measurement of the quantum metric tensor and related topological phase transition with a superconducting qubit, *Phys. Rev. Lett.* **122**, 210401 (2019).
- [55] M. Yu, P. Yang, M. Gong, Q. Cao, Q. Lu, H. Liu, S. Zhang, M. B. Plenio, F. Jelezko, T. Ozawa, N. Goldman, and J. Cai, Experimental measurement of the quantum geometric tensor using coupled qubits in diamond, *National Science Review* **7**, 254 (2019).